

NiCrSiB Thermal Sprayed Coatings Refused under Vibratory Treatment

Jelena ŠKAMAT^{1*}, Algirdas Vaclovas VALIULIS¹, Krzysztof Jan KURZYDŁOWSKI²,
Olegas ČERNAŠĖJUS¹, Raimonda LUKAUSKAITĖ¹, Marta ZWOLIŃSKA²

¹ Vilnius Gediminas Technical University, J. Basanavičiaus 28, LT-03224 Vilnius, Lithuania

² Warsaw University of Technology, Woloska 141, 02-507, Warsaw, Poland

crossref <http://dx.doi.org/10.5755/j01.ms.19.4.3386>

Received 25 January 2013; accepted 01 August 2013

The influence of mechanical vibrations on microstructure and some properties of Ni-based thermally sprayed and fused coatings deposited on a steel substrate has been studied. Self-fluxing powder with about 67 % Ni was used as a sprayed material. As-sprayed coatings were refused using conventional flame technique and with introducing of mechanical vibrations. During investigation of coatings by different methods it was found that vibratory treatment influences the solidified microstructure, corrosion resistance, microhardness, and surface state. It was found that in addition to thin planar solidification layer, obtained near the interface in conventional coatings, vibrations promote the forming of relatively thick boride-free layer. Several possible mechanisms are presented. Corrosion resistance tends to be improved with increasing of amplitude or frequency of vibratory treatment. The application of vibrations in set range has also allowed reducing coatings roughness up to 3 times. Comparison of results showed that vibrations amplitude proved as more effective parameter of vibratory treatment.

Keywords: thermal spray, NiCrBSi-system alloy coating, vibratory treatment, coating, and microstructure.

1. INTRODUCTION

Protective coatings technologies undoubtedly are one of the underlying areas of materials development. The separate group of technologies, called “thermal spraying”, is based on the melting and further deposition of solid materials on the preliminarily prepared surface in a form of dispersed jet. A wide range of used materials enables application of such technologies in the various industrial sectors. Nowadays thermal spraying is a high-tech branch of world economy with an annual turnover of about 5 billion USA dollars [1]. A fair share of works is carried out with using flame spray method. Numbers from 12 % (in Japan) to 30 % (in China) are given in source [1], and 30 % (in Germany) is given in source [2]. The present work is made on coatings produced using flame spraying-remelting technique.

In the particular case when wear and corrosion resistance at low and moderate temperature is required, the use of self-fluxing nickel-based alloys has received widespread use [3]. The formation of protective coating using such type of alloys normally is performed by two-steps process: deposition (spraying) of initial material (usually powder) and subsequent or simultaneous remelting of as-sprayed layer. The remelting enables to increase the density of sprayed layer by eliminating pores and cavities, inevitably formed in the as-sprayed layer, and to create strong metallurgical bond between the coating and the substrate. Under optimal remelting parameters and using proper ratio of alloying elements the uniform coatings, having minimal quantity of defects, and set special properties are obtained. Processes such as deoxidation, degassing, nucleation and growth of grains

are occurred during the remelting. The final coatings structure as well as properties in large degree depends on the efficiency of these processes.

Since the remelting of coatings is similar to the melting of compact alloys, some structure affecting methods, known and applied in the metallurgy, can be also effectively used in the technology of remelted coatings. In this case it's a question of use of vibratory treatment during remelting of sprayed layer in order to improve the microstructure and the performance of coatings by controlling the solidification processes.

Years of 1959 [4] and 1962 [5] are usually mentioned as a beginning of history of vibrations using in the metal casting. Firstly, in 1959 Ornitz had discovered that vibratory treatment during solidification can reduce casting inhomogeneity [4]. Later, in 1962 Patton had patented the same method to provide metal castings of refined-grain structure and for generally improving other metallurgical properties [5]. Frequencies of 10 kHz and above were used in the first case and range from 10 Hz to 1000 Hz was noted as preferable in the second. In other work [6] vibrations of frequencies 20 Hz and 100 Hz and of amplitudes 500 μm and 600 μm were used during casting of bronzes. The grain refinement effect and density increasing were obtained; the significant improving of mechanical properties such as tensile strength (from 20 % to 34 %) and elongation (from 15 % to 26 %) was established too. The positive effects of vibrational treatment are also reported in more recent works made on casting of aluminum alloys [7, 8].

However, the influence of vibratory treatment is not so unambiguous. Thus, it was showed in [9] what, in contrast to mentioned positive effects, the application of vibrations during solidification of Al-Si alloys LM6 and LM25 increased the size and amount of pores, and produced large holes on the top of the ingot.

*Corresponding author. Tel.: +370-52-744741; fax: +370-52-745043.
E-mail address: jelena.skamat@vgtu.lt (J. Škamat)

There are also publications on the application of vibratory treatment in coatings technology. Lateral vibrations of parameters 75 Hz and 197 μm are reported in [10] as most effective in porosity reduction (up to an 80 %) and homogenization of LPD (laser powder deposited) coating microstructure. Plasma cladded coatings produced under vibratory energy were improved in work [11] due to dispersion strengthening, grain refining strengthening, and solution strengthening (by increasing of solutes solubility). In result both microhardness and wear resistance of the coating were significantly promoted by mechanical vibration. Perpendicular vibrations of frequencies 50, 100, and 150 Hz with constant amplitude of 90 μm have been applied, and the best results were reached under 100 Hz frequency.

There are also a lot of works made on weld technology with application of vibratory treatment mostly as the means to relief residual stresses [12–14], what also is in the field of scientific interest for coatings creators, because residual stresses influence coating's performance in general and fatigue life in particular. As the main parameter, working amplitude in this case is reached when weldment under vibration is approaching to the resonance. Thus, the corresponding frequency has the value, specific to this system. For example, in work [13] vibrations, used for weldment stress relief, had frequencies of 79.6 Hz, 83 Hz, and 84.4 Hz. Grain refinement is declared by patentee of the used method [15]. However, in [13] the microstructure of specimens after stress relief showed increasing of grain size.

So, results of many researches testify vibratory treatment efficiency in controlling of solidification processes. Application of vibrations of proper parameters enables improving the microstructure and the performance of materials under the treatment. However, it must be noted that input of vibration energy can lead to contrary effects.

There are also a lot of works, made on metallurgy and coatings technology with using of ultrasound vibrations [16–19]. The ultrasound is not the novelty in materials engineering. The most common ultrasound effects, obtained in different materials engineering areas, have been described for example in [19]. Electrodeposition is one of the coatings technologies, where the using of power ultrasound allows to reach complex properties improving: increasing of adhesion, density, and hardness, reducing of porosity, improving of performance, etc. [16–19]. In thermal spray technology it's not used so widely, most likely due to peculiarity of ultrasound equipment and introducing of ultrasound vibrations.

Present work is a follow-up of multi-year research, which was begun in order to discover all possible effects of vibratory treatment on the microstructure and properties of Ni-based coatings deposited by flame spray-fuse technology. In order to determine a range of significant impact primary fusing experiments [20] had covered a large range of frequencies: 20 Hz, 100 Hz, 200 Hz, 1000 Hz, 2000 Hz, and 10 kHz. The coatings with the expressed grain-type structure were investigated and the reducing of grain size, slight increasing of hardness, and improving of coating wear resistance were obtained. The present work is made on coatings with high amount of inclusions firstly in order to analyse influence of vibrations on their size, shape, distribution, etc., because exactly morphological parameters

are what is reported in most of works as being affected by vibration energy. Also, since specimens, fused under vibration of frequencies 100 Hz and 200 Hz, showed the most significant results in [20], further experiments, being reported in present paper, were carried out using more narrow frequencies diapason, with choosing of parameters, allowing evaluating of vibration frequency impact on coating microstructure as well, as the impact of amplitude.

2. EXPERIMENTAL DETAILS

Commercial self-fluxing Ni-based alloy powder RW12497 from Castolin Eutectic with about 67 % Ni (Table 1) was used as spraying material. Powder was deposited on mild carbon steel plates of size (100×100×10) mm by oxy-fuel flame spraying. The preparation of substrate and spraying were performed according to recommendation of producer of powders and spraying/fusing tools (Rototec 80/CastoFuse torch from Castolin Eutectic). The main parameters of process are listed in Table 2. In order to make the same spraying condition for each specimen, robotic equipment Motoman 100 was used. After, as-sprayed layers were remelted in air by heating up to about 1100 °C with neutral oxy-acetylene flame. Several series of specimens were fused under vibratory treatment and one series was fused without vibration using standard fusing procedure. The range of vibrations has been selected being based on results of some primary experiments [20]. The mechanical vibrations of three frequencies 100 Hz, 150 Hz, and 200 Hz with constant amplitude of 25 μm , and vibrations with constant frequency of 100 Hz with changing of amplitudes from 25 μm to 115 μm (Table 3) were introduced parallel to coating surface, during fusing and during cooling till coating temperature reached 500 °C.

Initial powders were investigated by scanning electron microscope (SEM Hitachi SU-70) using magnification of ×200, ×700, and ×1500, and by energy dispersive X-ray microanalysis (EDS).

Table 1. Chemical composition of consumed powders (in wt.%)

Ni	Cr	Fe	B	Si	C	Cu	Mo
bal	15.7	2.72	3.92	4.11	0.45	1.94	4.69

Table 2. Preparation of substrate and spraying parameters

Preparation of substrate	Cleaning with degreasing agent. Grit blasting, preheating
Spraying flame	Neutral oxy-acetylene
Spraying distance, mm	150
Spraying rate/step/passes	250 mm/s / 5 mm / 8
Average thickness of as-sprayed layer	1.2–1.3 mm

Table 3. Parameters of vibration condition and samples marking

Frequency, Hz	Amplitude, μm				
	0	25	50	75	115
0	NV				
100		100_25	100_50	100_75	100_115
150		150			
200		200			

The thermal study of powders was accomplished through differential thermal analysis (DTA), which was carried out with DTA/DSC SETARAM LABSYS equipment. 50 mg of powder was placed in alumina crucible and during non-isothermal experiment was heated in argon (5N) atmosphere from ambient temperature to 1250 °C. The heating rate was 50 °C/min for temperature range from ambient to 750 °C, and 10 °C/min for temperature range from 750 °C to 1250 °C. Temperature difference between sample and reference, inert in this thermal cycle, was recorded and plotted against heating temperature.

The microstructure of sprayed-fused coatings was observed on etched transverse cross-sections using scanning electron microscope SEM HITACHI SU-70. EDS/WDS analyzers and the necessary software were used in order to perform point microanalysis, linear microanalysis or chemical mapping of the surface under examination.

The phase analyzes were done on Philips X-ray powder diffractometer equipped with X-Pert goniometer. Graphite-monochromatized $\text{CuK}\alpha$ ($\lambda = 0.1541837$ nm) radiation was used in all examined cases. Experimental conditions were as follows: voltage valued 40 kV and the current value was 40 mA, angle range 2θ : 20°–120°, step $\Delta 2\theta - 0.05$, exposure time per step – 3 s. The phase structure comparison of vibrated and unvibrated samples was carried out on XRD patterns through comparison of peaks disposition and intensity.

The thickness of layers was measured on SEM micrographs of cross-sections using ScionImage software. The measurement was repeated 5 times for each specimen.

Microhardness measurements have been done by Knoop method using Zwick Roell ZH μ tester with a 500 g load. Measurements were performed on polished cross-sections, each specimen was measured 10 times and the average values are presented here.

Electrochemical corrosion tests were accomplished through potentiodynamic measurements carried out using potentiostat/galvanostat AutoLab PGSTAT32N. A three-electrodes cell arrangement was used, with a saturated calomel reference electrode as a reference electrode and a platinum wire as the auxiliary electrode. Two solutions were used: 3.4 % NaCl solution, naturally aerated at 21 °C, and 0.1 M H₂SO₄ solution, naturally aerated at 21 °C. Potentiodynamic polarization scans were carried out with a scan rate of 0.5 V/s in range of potential from –1500 mV to 180 mV using 3.4 % NaCl solution, and with a scan rate of 1 V/s in range of potential from –700 mV to 1500 mV in 0.1 M H₂SO₄ solution. Measurements were performed on polished tops of coatings.

Roughness measurements were carried out with using of tester TR200. Surfaces of remelted coatings after cleaning with isopropyl alcohol were measured 3 times each, and values of R_a parameter are presented here.

3. RESULTS AND DISCUSSION

Firstly powders were examined with SEM and EDS. Nominally powders consist of spherical grains having grain diameter of 38 μm –125 μm , but really it was found that part of powder particles has irregular shape or the shape of coalesced spheres. X-ray microanalysis using EDS showed that powders are represented like a one-type

particles of Ni-based alloy. Higher magnification showed that particles have the fine crystal structure of primary solidification (Fig. 1).

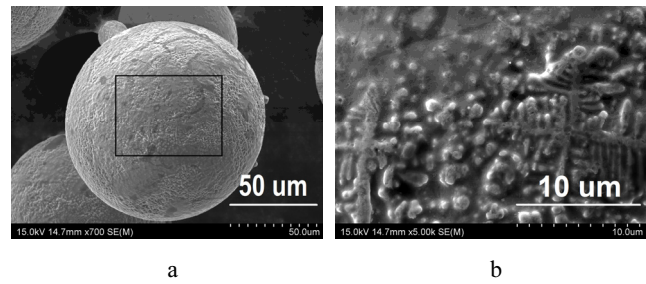


Fig. 1. SEM micrograph of initial powder (a) and denoted area (b)

In order to optimize thermal cycle of refusing process, and to avoid overheating of as-sprayed layers in the process of refusing, the thermal study of powders was carried out. Two endothermic melting peaks of 1023 °C and 1102 °C, recorded on curve (Fig. 2), denote the temperatures of most intensive melting of powders in this temperature range. The remelting technique of as-sprayed layers was prepared based on these results.

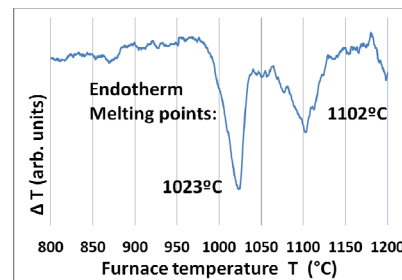


Fig. 2. Endothermic melting peaks of Ni-based alloyed powders

After remelting, microstructure of sprayed-fused coatings was investigated and specimens, produced under vibratory treatment, were compared with unvibrated reference. Unfortunately, absolutely correct phase analysis by XRD was impossible because every peak can correspond to more than one phase of the same elements with different stoichiometric compositions. XRD pattern of unvibrated coating is presented on Fig. 3. Only five phases have been established with a high probability: $\text{Cr}_{1.12}\text{Ni}_{2.88}$, $\text{Fe}_{1.34}\text{Si}_{0.66}$, Ni_3B , NiSi_2 , and Fe_3Ni_2 . The further structure analysis was accomplished using SEM and X-ray microanalysis. It was found that remelted coatings microstructure consists of soft metallic 2-phase matrix, hardened by high amount of hard inclusions of three types at least – most likely by carbides of type M_{23}C_6 and M_7C_3 , and by borides of type M_2B . The fragment of the microstructure including all obtained phases is presented on Fig. 4. Based on the results of XRD patterns identification and X-ray point microanalysis, linear microanalysis, and mapping, light grey areas, denoted on micrograph as 1, were identified as γ -Ni solid solution and grey areas around (denoted as 2 on micrograph) were identified as Ni/Ni-B eutectic. Point X-ray microanalysis in different areas of cross-section showed, that the amount of elements, dissolved in γ -Ni solid solution, can vary. However, this difference is not so significant and average amount of elements is about 8 % Cr, 8.5 % Si, 3 % Cu, 0.3 % Mo, and 4 % Fe.

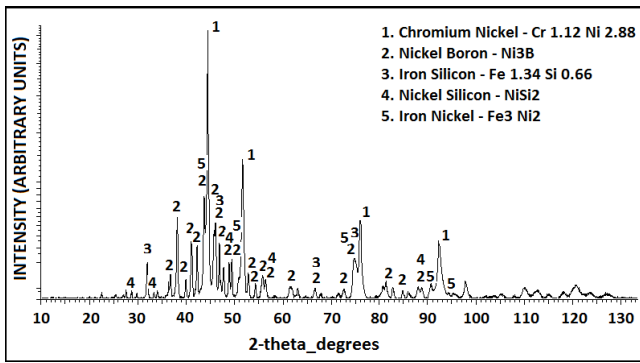


Fig. 3. XRD pattern of unvibrated coating

Metal part in boride phase (dark precipitations denoted as 3 on Fig. 4) is represented mostly by Cr and, to a lesser extent, by Mo. The total amount of other elements such as Ni, Fe, and Si didn't exceed three per cent. So, boride phase was identified as a complex junction of type $(CrMo)_2B$. Besides Cr and C, X-ray point microanalysis and chemical mapping showed also presence of significant amount of Ni, Si, and Mo in $M_{23}C_6$ type inclusions, and significant amount of Ni in a carbides phase of type M_7C_3 . Consequently, these hard inclusions were identified as a complex carbides of types $(CrNi)_7C_3$ and $(CrNiSiMo)_{23}C_6$. These phases are denoted on SEM micrograph below (Fig. 4) respectively as 4 (dark grey inclusions) and 5 (white inclusions).

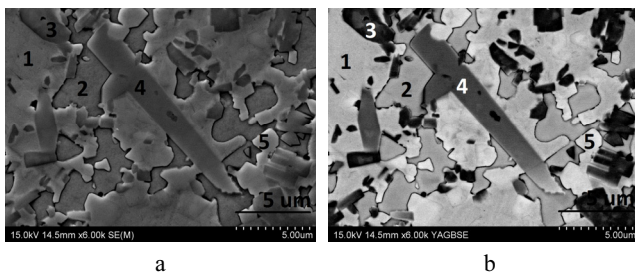


Fig. 4. SEM micrographs including main identified phases in remelted layer: a – secondary electron SE image; b – backscattered electron BSE image; 1 – γ -Ni solid solution; 2 – Ni/Ni-B eutectic; 3 – M_2B borides; 4 – M_7C_3 carbides; 5 – $M_{23}C_6$ carbides

Analysis of phase structure and morphology depending on powder chemical composition is presented in [21]. Presence of Ni solid solution, nickel and chromium borides, chromium carbides, and nickel silicides, is observed in a most of alloys, investigated in this work. The similar phases are reported in works [22–24]: Ni, Ni_3B , CrB, Cr_7C_3 , $(Cr,Fe)_7C_3$, Cr_7C_2 , Cr_3C_2 . Different deposition and refusing techniques were used in mentioned works, however phases, observed in different alloys, are similar, what can testify weak influence of refusing conditions on the formation of main phases. On the other hand, some powders, being reported in mentioned works, have chemical composition similar to the powder, used in presented work; however phases of $M_{23}C_7$ and M_2B are not reported there. Other authors have reported in their work [25] presence of phases such as $\gamma(Ni, Fe)$ solid solution, M_7C_3 , $M_{23}C_6$, and Cr_2B . Application of Rietveld refinement method to analyze of XRD spectra increases the reliability of these results. Besides, several references are also specified in [25] as being similar to obtained

results. Phases identified in the present work are in good correspondence with [25] and in general are typical for such type of coatings.

The analysis of phase structure on XRD patterns didn't show any visible differences for vibrated and unvibrated coatings. Absence of any influence of vibrations on phase structure is noted by most of authors.

The main microstructural differences, being reported in the most of works, regard the size, the morphology, and the distribution of precipitates. In the present work segregations of different types of hard precipitates have formed zonal-type structure. As it can be seen on Fig. 5, the structure is represented as alternation of typical zones (denoted 1, 2, and 3 on Fig. 5, a) with the average size about $250 \mu m^2$. The zone 1 can be characterized as area of soft metal matrix hardened by low amount of $M_{23}C_6$ type inclusions, placed in Ni solid solution. In zone, denoted 2, presence of dark borides inclusions was established besides white carbides. Carbides of $M_{23}C_6$ type and of M_7C_3 type was found in zone 3. Areas, including all types of precipitates, were also met during observation of coatings microstructure. It can be noted, that $M_{23}C_6$ carbides, obtained in all zones, are distributed most uniformly.

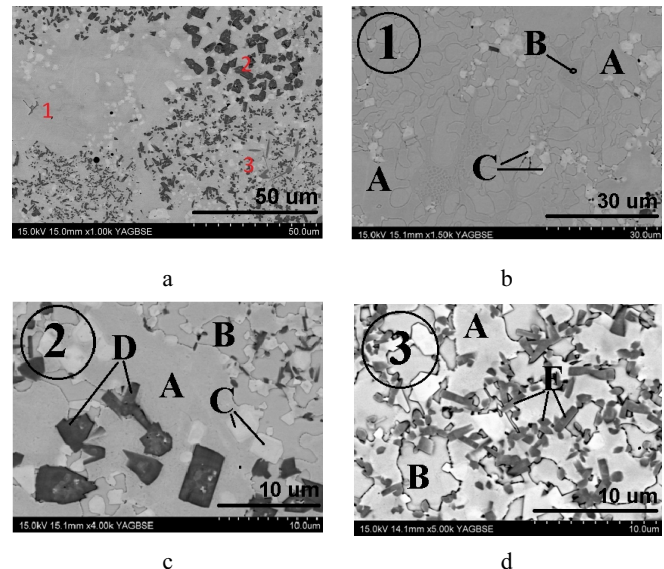


Fig. 5. SEM micrograph of cross-section area, including 3 different zones (backscattered electron BSE image) (a) and zones, denoted as 1, 2, and 3 (b, c, d); A phase – γ -Ni solid solution; B phase – Ni/Ni-B eutectic; C – $M_{23}C_6$ carbides; D – M_2B borides; E – M_7C_3 carbides

Visually determined zones repeat the shape of powder particles. Since after deposition the most of powder is incorporated in coating as separated particles with no changes of their shape, the size difference of powder particles can influence zonal-type character of microstructure. In this case the bigger particles require longer heating for reaching proper refusing temperature, while the smaller particles can be already overheated. Zonal-type structure as well as wide varying of precipitates size, established in vibrated coatings as well as in unvibrated reference, can be also explained by peculiarity of flame remelting technique, when the same area of layer to be refused can be affected by "walking" flame heat several times.

Structure inhomogeneity was also established in vertical

direction – during observation of layers from the interface to the top. The solidification starts from the interface, where the substrate acts as a heat sink, with the forming of thin nearly one-phase layer, consisting of Ni solid solution with occasional inclusions of eutectic (Fig. 6).

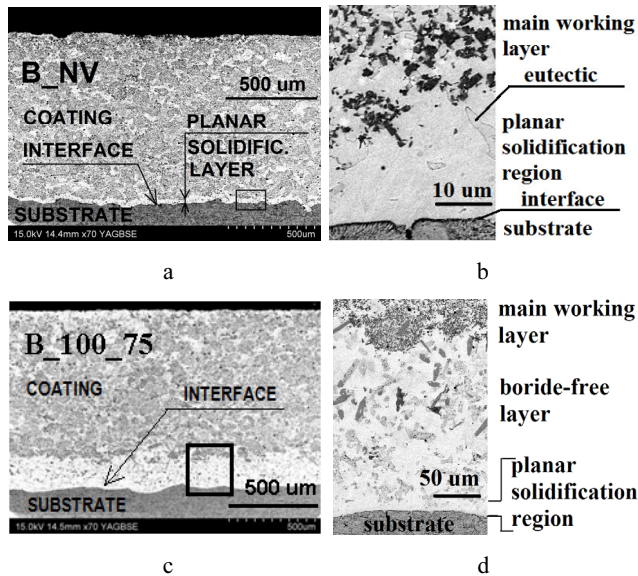


Fig. 6. SEM micrograph (backscattered electron BSE image): a – transverse cross-section of unvibrated coating and denoted area (b); c – transverse cross-section of coating, vibrated under 100 Hz 75 μm vibrations and denoted area (d)

Planar nature of solidification is explained by peculiar solidification conditions in this region, in particular high temperature gradient (G) and slow solidification velocity (V). According to [26,27] sufficiently high G/V ratio promotes planar crystallization. The average thickness of planar solidification layer in vibrated and unvibrated coatings is similar (about 40 μm). In unvibrated coating this monolayer gradually is changed by main layer, containing all obtained phases described earlier. Thin outer layers of all coatings show the increasing of inhomogeneity mostly due to increasing of size and shape varying of hard inclusions. In vibrated coatings relatively thick layer, free from borides and including large-size carbides of both types, is formed immediately above the layer of planar solidification. Since the boundary between these layers is not expressed so clearly, the thickness was measured from the substrate-coating interface.

Results presented on Fig. 7 and Fig. 8 show that the thickness of “borides-free” layer varies with changing of vibration frequency as well as with changing of amplitudes. The application of vibrations of frequency 100 Hz and of amplitude 25 μm have led to the forming of “borides-free” layer with joint thickness of 127 μm. The thickness was enlarged to 136 μm with increasing of amplitude till 50 μm and have reached the maximum (237 μm on the average) under amplitude of 75 μm. Further increasing of amplitude has led to the wane of layer. The increasing of frequency till 150 Hz and 200 Hz didn't promote the forming of layer so significantly. In contrast, the thickness of “borides-free” layer was reduced in result, but, anyway, has remained above the thickness of planar solidification layer in unvibrated coating.

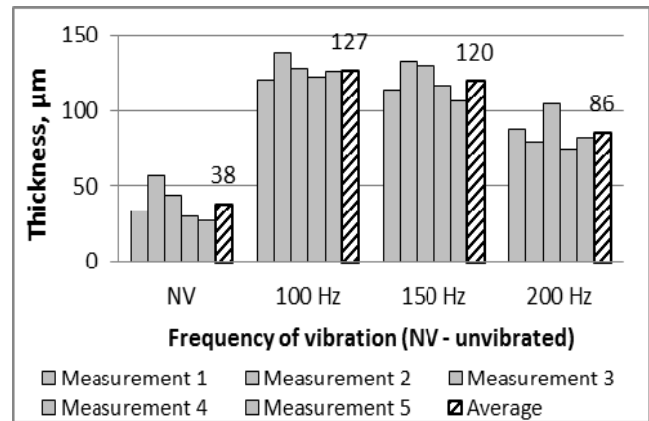


Fig. 7. Thickness of “borides-free” layer in coatings remelted under constant amplitude of 25 μm (for unvibrated reference NV the thickness of planar solification layer is presented)

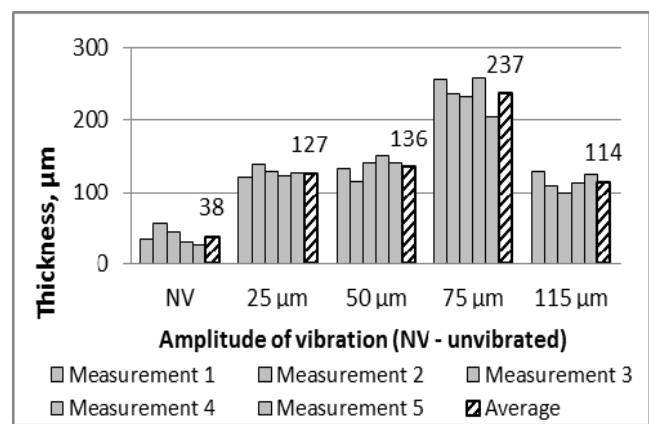


Fig. 8. Thickness of “borides-free” layer in coatings remelted under constant frequency of 100 Hz (for unvibrated reference NV the thickness of planar solification layer is presented)

Usually increasing of structure homogeneity and uniformity of precipitation distribution is preferable. Apparently, in this case vibratory treatment has led to contrary effect and has form thick borides-free layer near interface. The microstructural changes usually are related to the changes in solidification condition. In [13] increasing of grain size due to convection modification by vibration energy is reported. In present work large-size inclusions predominance in borides-free layer can testify the change in solidification process caused by convection modifying to conditions, when the amount of spontaneous crystallization nucleus is limited. The wave extending during vibrating may also promote the growing of inclusions by destroying of the part of crystallization centres. However, neither of mechanisms explains the absence of borides in the near interface layer for sure. Since boron is one of the lightest elements, densimetric movement of boron atoms or borides seems as to be the most probable here. Microhardness measurements results showed that average microhardness of vibrated coatings was increased and the thicker borides-free layer was obtained near interface, the higher microhardness value was determined in main layer (Fig. 9). At the same time the microhardness of borides-free layer has the value intermediate between the microhardness of substrate and

the microhardness of main coatings' layer (Fig. 10). Accordingly, application of vibratory treatment of proper parameters lead to the forming of coatings with harder outer layers, whereas the formation of softer layer near interface can promote more uniform distribution of residual stresses. On the other hand, if the increasing of coatings microhardness is reached due to the increasing of precipitations amount in upper layers, this effect can be accompanied by the wane in corrosion resistance, since this property is provided mainly by Cr-rich Ni-based metal matrix.

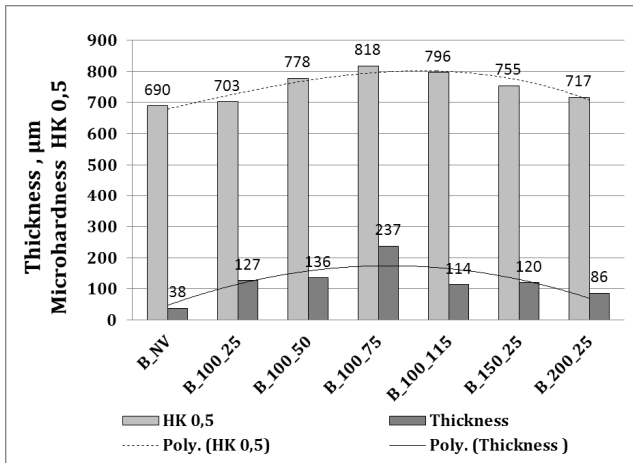


Fig. 9. Borides-free layers thickness in comparison with average microhardness, measured in the main part (600 µm from the interface) of remelted coatings

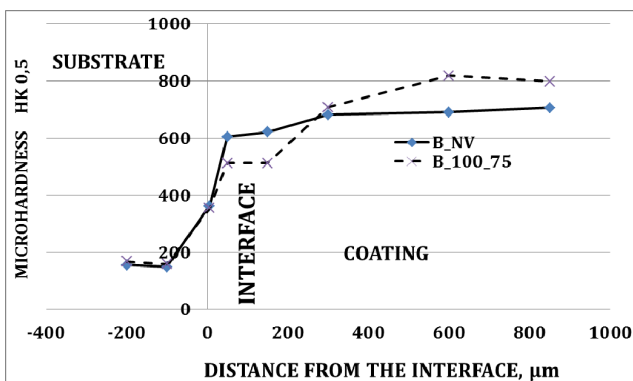


Fig. 10. Microhardness distribution in remelted layers

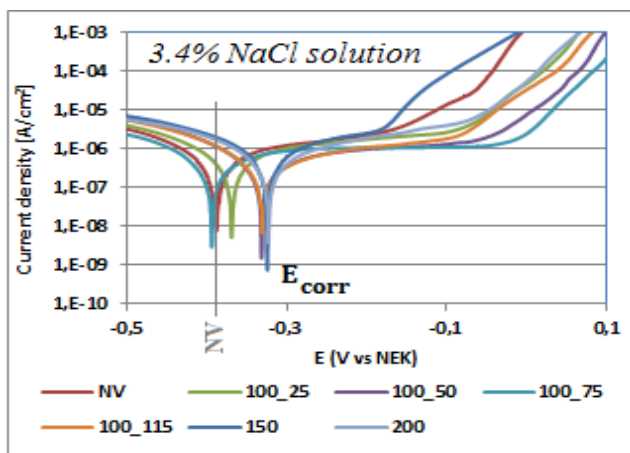


Fig. 11. Potentiodynamic polarization curves recorded in 3.4 % NaCl solution

In order to evaluate impact of obtained microstructure changes on coatings behaviour in corrosive environments some corrosion tests were carried out. The method of potentiodynamic polarization was chosen as express test allowing showing even the small difference in corrosion mechanism and in materials behaviour in particular medium. Solutions were chosen considering typical operating conditions for such type of coatings. The one of the main advantages of Ni-based coating is equally good corrosion resistance in both environments acid and alkaline: for example in seawater or in sulphuric acid vapour. So, 3.4 % NaCl solution and 0.1 M H₂SO₄ solution were used for measurements.

Polarization curves recorded in NaCl solution are presented on Fig. 11. The shapes of the curves obtained for all samples are very similar, what shows the analogy of corrosion processes for all samples and indicates that the arrangement of layers on substrate does not affect on their progress in the solution significant. Surfaces become spontaneously passive in the test NaCl solution. However, further potential increasing leads to systematic increasing of current density. Of all of tested specimens unvibrated and “100_75” samples showed the weakest corrosion resistance, as their peaks correspond to the least corrosion potential of -0.3877 mV for NV specimen and -0.3941 mV for 100_75 specimen (Table 4). The worse corrosion test result of “100_75” specimen can be, probably, related with theoretical increasing of hard precipitations amount. However, the differences in corrosion potential E_{corr} for two these specimens are very small, and it can be noted that, in the set range, vibrations of parameters of 100 Hz and 75 µm most intensely promote forming of harder outer layers without impact on corrosion resistance. Having excluded the result of “100_75” from a general series it can be noted also that application of vibrations as well as the increasing of the amplitude or frequency lead to the shift of corrosion potential to more positive area, what indicates the improving of corrosion stability in this solution. Very close results of about -0.33 mV were obtained on four specimens: “100_50”, “100_115”, “150”, and “200”. Since no changes in phase structure and morphology were obtained during microstructural analysis the reason, caused improving of corrosion resistance, remains uncovered. Having in mind all vibratory treatment effects reported by other authors, it can be assumed that vibration energy has relieved the general level of residual stresses, what have slightly impacted samples behaviour in corrosive medium. Two specimens (unvibrated and “150”) were also tested in H₂SO₄ solution. The effect of corrosion potential increasing with application of vibratory treatment was obtained also, but the further research is necessary.

Table 4. Potential of corrosion in 3.4 % NaCl solution

Sample	E_{corr} [mV _{NEK}]
NV	-0.3877
100_25	-0.3694
100_50	-0.3317
100_75	-0.3941
100_115	-0.3299
150	-0.3244
200	-0.3232

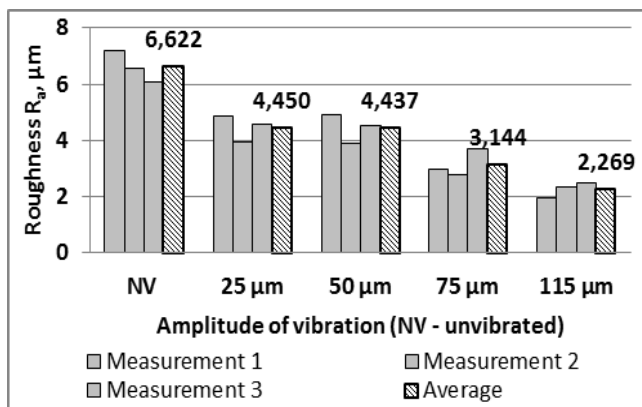


Fig. 12. The influence of amplitude on coatings surface roughness R_a after remelting under constant vibration frequency of 100 Hz

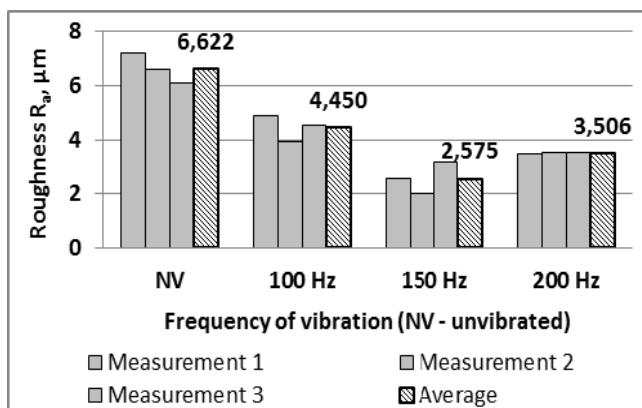


Fig. 13. The influence of frequency on coatings surface roughness R_a after remelting under constant vibration amplitude of 25 μm

Evaluating of coatings surface state after remelting was carried out through the measurement of roughness. Results are presented as the dependence of R_a parameter from the vibration amplitude (Fig. 12) and from the vibration frequency (Fig. 13). All specimens produced under vibratory treatment can be characterized as having smoother surface in comparison with unvibrated reference. Application of vibrations of the lowest parameters (100 Hz and 25 μm) enabled to reduce R_a parameter about 30 % (from 6.622 μm to 4.450 μm). Further increasing of amplitude under constant frequency of 100 Hz was accompanied by degression of R_a parameter. Specimen remelted under maximum amplitude of 115 μm showed the smoothest surface with R_a value of 2.269 μm , what is about 3 times less than R_a value of unvibrated sample. Also surface roughness was significantly reduced with the increasing of frequency from 100 Hz to 150 Hz (with constant amplitude of 25 μm). However it was the minimum and further rising of frequency lead to the increasing of roughness.

4. CONCLUSIONS

Several conclusions can be drawn based on results of this work.

First of all, the using of vibratory treatment during remelting of as-sprayed Ni-based coatings influences the microstructure, corrosion behaviour, microhardness, and surface state.

In coatings with high amount of hard inclusions, vibrations promote forming of boride-free layer near interface, most probably due to densimetric movement of particles (or atoms) up - towards a surface. No changes in phase composition were found during comparison of vibrated and unvibrated coatings. Corrosion testing results showed that this effect can be used for creating of hardened outer layer without losing of corrosion resistance.

It was found also that vibratory treatment in the set parameters range allows roughness reducing up to 3 times. Due to this effect the material loss during coating finishing processing can be significantly reduced. It's also important factor when no grinding or other finishing operation is used after refusing, since surface roughness is one of the major factors that influence wear and corrosion rates [28].

Thus, in the tests covered by the presented research, vibratory treatment proved as the method, allowing structure modifying and performance improving of reusable coatings. However, comparison of the results showed that vibrations parameters corresponding to the maximum effect differ for various properties. The maximum complex influence can be reached by selection of some intermediate parameters. It was found also that change of amplitude yields similar or better result, than frequency change, what determines amplitude as more effective parameter in this range.

Acknowledgments

Potentiodynamic polarization measurements was carried out within a NANOMET Project financed under the European Funds for Regional Development (Contract no. POIG. 01.03.01-00-015/08).

REFERENCES

1. **Korobov, J.** International Thermal Spray Conference and Exposition ITCS 2010: Review and Analysis. Thermal Spray – Modern Situation. Materials of International Scientific and Practical Seminar (28th–29th of September, 2010), Yekaterinburg, 2010: pp. 4–24. Available online at <http://urfu.ru>
2. **Bach, F.-W., Laarmann, A., Wenz, T.** (eds). Modern Surface Technology. Germany, 2006: 325 p. <http://dx.doi.org/10.1002/3527608818>
3. **Kim, H.-J., Hwang, S.-Y., Lee, Ch.-H., Juvanon, P.** Assessment of Wear Performance of Flame Sprayed and Fused Ni-based Coatings *Surface and Coating Technology* 172 2003: pp. 262–269.
4. **Ornitz, N.** Metal Casting. US patent No. 2897557, 1959.
5. **Patton, A.** Metal Casting. US patent No. 3045302, 1962.
6. **Pogodin-Aleksejev, G.** Ultrasound and Low Frequency Vibrations in Alloy Casting. Moscow, 1961: 83 p.
7. **Taghavi, F., Saghafian, H., Kharrazi, Y. H. K.** Study on the Effect of Prolonged Mechanical Vibration on the Grain Refinement and Density of A356 Aluminum Alloy *Materials and Design* 30 2009: pp. 1604–1611. <http://dx.doi.org/10.1016/j.matdes.2008.07.032>
8. **Chirita, G., Stefanescu, I., Soares, D., Silva, F. S.** Influence of Vibration on the Solidification Behavior and Tensile Properties of an Al-18 wt% Si Alloy *Materials and Design* 30 2009: pp. 1575–1580. <http://dx.doi.org/10.1016/j.matdes.2008.07.045>

9. **Kocatepe, K.** Effect of Low Frequency Vibration on Porosity of LM25 and LM6 Alloys *Materials and Design* 28 2007: pp. 1767–1775.
<http://dx.doi.org/10.1016/j.matdes.2006.05.004>
10. **Foroozmehr, E., Lin, D., Kovacevic, R.** Application of Vibration in the Laser Powder Deposition Process *Journal of Manufacturing Process* 11 2009: pp. 38–44.
11. **Wang, S., Li, H., Chen, X., Chi, J., Li, M., Chai, L., Xu, H.** Improving Microstructure and Wear Resistance of Plasma Clad Fe-based Alloy Coating by a Mechanical Vibration Technique during Cladding *Materials Science and Engineering A* 528 2010: pp. 397–401.
<http://dx.doi.org/10.1016/j.msea.2010.09.021>
12. **Jurčius, A., Valiulis, A. V., Černašėjus, O.** Influence of Vibratory Stress Relief on Residual Stresses in Bridge Structural Members Weldments *The Baltic Journal of Road and Bridge Engineering* 4 (6) 2011: pp. 243–248.
13. **Jurčius, A.** Effect of Vibratory Treatment on Residual Stresses in Structural Steel Weldments. Doctoral Dissertation. Vilnius: 2010.
14. **Aoki, S., Nishimura, T., Hiroi, T.** Reduction Method for Residual Stress of Welded Joint Using Random Vibration *Nuclear Engineering and Design* 235 (14) 2005: pp. 1441–1445.
15. Grain Refinement Achieved by Applying Meta-Lax Technology during Welding. Available online at <http://www.meta-lax.com>
16. **Zanella, C., Lekka, M., Bonora, P. L.** Effect of Ultrasound Vibration during Electrodeposition of Ni-SiC Nanocomposite Coatings *Surface Engineering* 26 (7) 2010: pp. 511–518.
<http://dx.doi.org/10.1179/174329409X438961>
17. **Zheng, H. Y., An, M. Z.** Electrodeposition of Zn-Ni-Al₂O₃ Nanocomposite Coatings under Ultrasound Conditions *Journal of Alloys and Compounds* 459 (1–2) 2008: pp. 548–552.
18. **Walker, C., Walker, R.** Effect of Ultrasonic Agitation on Some Properties of Electrodeposits *Electrodeposition and Surface Treatment* 1 (6) 1973: pp. 457–469.
[http://dx.doi.org/10.1016/0300-9416\(73\)90029-1](http://dx.doi.org/10.1016/0300-9416(73)90029-1)
19. **Abramov, O., Horbenko, I., Shveglja, Sh.** Ultrasound Treatment of Materials. Moskva, 1984: 280 p. (in Russian).
20. **Škamat, J., Valiulis, A. V., Černašėjus, O.** The Influence of Mechanical Vibrations on Properties of Ni-based Coatings *Journal of Vibroengineering* 12 (4) 2010: pp. 604–610.
21. **Lebaili, S., Durand-Charre, M., Hamar-Thibault, S.** The Metallurgical Structure of As-solidified Ni-Cr-B-Si-C Hardfacing Alloys *Journal of Materials Science* 23 1988: pp. 3603–3611.
<http://dx.doi.org/10.1007/BF00540502>
22. **Kim, H.-J., Hwang, S.-Y., Lee, Ch.-H., Juvanon, Ph.** Assessment of Wear Performance of Flame Sprayed and Fused Ni-based Coatings *Surface and Coatings Technology* 172 2003: pp. 262–269.
23. **Gonzalez, R., Garcia, M. A., Penuelas, I., Cadenas, M.** Microstructural Study of NiCrBSi Coatings Obtained by Different Processes *Wear* 263 2007: pp. 619–624.
24. **Gomez-del Rio, T., Garrido, M. A., Fernandez, J. E., Cadenas, M., Rodriguez, J.** Influence of the Deposition Techniques on the Mechanical Properties and Microstructure of NiCrBSi Coatings *Journal of Materials Processing Technology* 204 2008: pp. 304–312.
<http://dx.doi.org/10.1016/j.jmatprotec.2007.11.042>
25. **Hou, Q. Y., Huang, Z. Y., Shi, N., Gao, J. S.** Effects of Molybdenum on the Microstructure and Wear Resistance of Nickel-based Hardfacing Alloys Investigated Using Rietveld Method *Journal of Materials Processing Technology* 209 2009: pp. 2767–2772.
26. **Kurz, W., Triverdi, R.** Rapid Solidification Processing and Microstructure Formation *Materials Science and Engineering* 179–180 1994: pp. 46–51.
27. **Navas, C., Colaco, R., de Damborenea, J., Vilar, R.** Abrasive Wear Behaviour of Laser Clad and Flame Sprayed-Melted NiCrBSi Coatings *Surface and Coatings Technology* 200 2006: pp. 6854–6862.
<http://dx.doi.org/10.1016/j.surfcoat.2005.10.032>
28. **Zhong, Z. W., Peng, Z. F., Liu, N.** Surface Roughness Characterization of Thermally Sprayed and Precision Machined WC-Co and Alloy-625 Coatings *Materials Characterization* 58 2007: pp. 997–1005.
<http://dx.doi.org/10.1016/j.matchar.2007.05.010>